Imidazolium decyl sulfate: a very promising selfmade ionic hydrogel

Oscar Cabeza[a], Esther Rilo[a], Luisa Segade[a], Montserrat Domínguez-Pérez[a], Sandra García-Garabal[a], David Ausín[a], Elena López-Lago[b], Luis Miguel Varela[c], Miguel Vilas[d], Pedro Verdía[d] and Emilia Tojo[d]

[a]Dpt. de Física e C.C. da Terra. Universidade da Coruña. 15071 A Coruña (Spain).
[b]Dpt. de Física Aplicada. Universidad de Santiago de Compostela. 15782 Santiago de Compostela (Spain)
[c]Dpt. de Física de Partículas. Universidad de Santiago de Compostela. 15782 Santiago de Compostela (Spain)
[d]Dpt. de Química Orgánica. Universidade de Vigo. 36310 Vigo (Spain)

How to cite

O. Cabeza, E. Rilo, L. Segade, M. Domínguez-Pérez, S. García-Garabal, D. Ausín, E. López-Lago, L. M. Varela, M. Vilas, P. Verdía and E. Tojo, Imidazolium decyl sulfate: a very promising selfmade ionic hydrogel, *Mater. Chem. Front.*, 2018, **2**, 505–513. DOI: 10.1039/C7QM00510E

Abstract

In this paper we show the synthesis, structural characterization, phase diagram and physical properties of the ionic liquid 1-ethyl-3-methyl imidazolium decyl sulfate [EMIm][DSO_4] for the first time. At 25 ºC it is a crystalline solid or a liquid depending on the thermal history, being its melting point about 33 ºC and its solidification one about 22 ºC. The interest of this new IL lies in its ability to become a rigid hydrogel when mexed with water. As many ILs, this one is hygroscopic and it adsorbs moisture to about 14 $_{wt}$% of water at usual laboratory conditions and up to 27 $_{wt}$% in a 100 % saturated atmosphere. Due to the H-bonds between water and the amphiphilic [DSO_4] anions, a lyotropic H_I liquid crystalline phase is formed in the hydrated state, as can be observed in the micrographs made with white polarized light. The moisture adsorption is a complete reversible process, thus the rigid-gel sample loses all adsorbed water when it is left in a dry atmosphere for some hours, transiting to liquid state. Phase diagram temperature-water concentration is presented and compared with that of the parent compound [EMIm] octyl sulfate, [OSO_4]. X-ray diffraction revels that below 15 ºC the hydrated compound crystallizes in a P2/m monoclinic. The structure of the new compound was confirmed by NMR, FTIR and mass spectroscopy (MS) . In addition, the temperature behavior of ionic conductivity was experimentally measured and analyzed for the pure compound and for two samples hydrated with 10 $_{wt}$% and 39 $_{wt}$% of water. Viscosity and density were also measured vs. temperature for the pure sample. This IL shows a great potential for many practical applications.

Introduction

In recent papers we published that the ionic liquid (IL) 1-ethyl-3-methylimidazolium octyl sulfate [EMIm][OSO_4], forms an ionic hydrogel at room conditions when mixed with water, named rigid-gel state[1,2]. Let us remember that hydrogels are crosslinked hydrophilic polymer assemblies classically made from high molecular weight biopolymers. In this work, the alkyl sulfate anion was enlarged two carbons and obtain the [EMIm][DSO_4], e.g. decyl sulfate; its properties have shown to be spectacular and present very interesting properties that can be used for many applications[3]. As known, sulfate salts with long chain alkyl chains, e.g. sodium dodecyl sulfate, are anionic surfactants and are known to form micellar aggregates in aqueous solution. Also ILs with long alkyl chains, as 1-dodecyl-3-methyl imidazolium bromide, present a similar character[4]. Such lyotropic mesophases are usually formed by adding amphiphiles to a solvent. Those form aggregates above the critical micelle concentration, which can have various shapes and sizes and constitute the building blocks of liquid crystals. Usually, the normal topology (or Type 1) phase structures forming upon increasing the amphiphilic concentration range from micellar cubic, via hexagonal and bicontinuous cubic to lamellar.[5] A further increase in amphiphilic concentration leads to the formation of inverse topology lyotropic (or Type 2) phases, where the polar domain is discontinuous. Thus, addition of water to long alkyl chain ILs to a composition containing from 5-40 $_{wt}$% results in a strong, anisotropic 2D pattern featuring two diffraction rings, which indicate the presence of a lamellar lyotropic liquid crystalline phase.[6] A characteristic optical texture of the birefringent sample in polarized light microscopy supports this finding. *Inoue et al.* have studied the binary mixture of 1-dodecyl-3-methyl imidazolium bromide and water by differential scanning calorimetry and polarized optical microscopy and found the hexagonal and the lamellar liquid crystalline phase.[4] A similar behaviour observed by SAXS has been reported for 1-hexadecyl-3-methyl imidazolium chloride.[7] *Russina et al.* have studied the water-free IL [EMIm][OSO_4] by SAXS.[8,9] The low *Q* peak in the SAXS pattern of this together with a range of similar ILs provide evidence for an intermediate range order existing in [EMIm][OSO_4], and other ILs[6,10] with a big difference in the nature and spatial extent of the interactions of heads and tails.

In our IL, to the lyotropic character of the decyl sulfate anion must be added the chromonic character of the [EMIm] cation, which will help to form tubular micelles due to their π-π interactions[11].

One of the most promising applications of ILs is to develop a new generation of electrolytes to substitute those actually used in electrochemical devices[12-14]. For this purpose, the alkyl sulfate ILs family is very suitable, and it has the advantage of being completely halide free[15]. For many electrochemical applications it is desirable to have a quasi-solid conductor instead of a liquid one, and many attempts have been performed to obtain them using ILs[16-25]. The usual ways to get it is to polymerize monomers mixed with an IL[16-18], to include a gelator in an aqueous mixture of a given IL[19-23], or even to polymerize the IL itself[24,25]. In majority of cases, the ionic conductivity drops abruptly in the quasi solid state with regard to its value when it is in liquid state[25], although ionic hydrogels usually do not, being that magnitude unaltered during phase transition[1,2,24]. In this paper the synthesis, structure and the temperature behavior of some physical properties of [EMIm][DSO_4] are presented. This material is a new IL never synthesized nor reported before, at our knowledge. When it adsorbs a tiny quantity of water from the atmosphere it becomes an ionic hydrogel where the biopolymer role is taken by the alkyl sulfate anion, and the chromonic character of the cation will help to form long tubular micelles[11]. This liquid crystalline mesomorphic state appears well above room temperature and, as mentioned, without the addition of any polymer or gelator. It is in that state up to 85 °C with the appropriate amount of water, at our knowledge this is the first IL based ionic hydrogel that is in a stable quasi-solid above 50 °C[1,14,20,24], because this one is. As mentioned, this IL adsorbs the necessary amount of water directly from the atmosphere, regulating its composition up to 27 $_{wt}$% of weight percentage in a 100 % relative humidity grade. This new compound has been recently patented[26]. The proposed applications for this new material are broad, including electrolytes,[12,13] gas sensors,[21] membranes[14] or catalysis[23,27].

Experimental

Chemicals

1-Methylimidazolium (Sigma-Aldrich, 99%), diethyl sulfate (Fluka, ≥99%), toluene (Merck, 99%), 1-decanol (Sigma-Aldrich, 99%), methane sulfonic acid (Aldrich, anhydrous) and *tert*-butyl methyl ether (Panreac, 99.5%), were used as received without any pre-treatment.

Synthesis

The ^{1}H and ^{13}C NMR spectra of the obtained ionic liquids were recorded on a Bruker ARX at 400.1621 and 100.6314 MHz respectively, with chemical shifts given in parts per million and coupling constants (J) in Hertz. The purity of the synthesized IL was determined by ^{1}H-NMR by using the parameters and methodology for qNMR measurement described by S. Mahajan et al.[28]. The internal standard employed was hydroquinone. ESI mass spectra were recorded on a micrOTOF Focus spectrometer and on an apex-Qe spectrometer. All spectral data were supplied by the Centre of Research Support (CACTI) of the University of Vigo

1-ethyl-3-methylimidazolium methyl sulfate [EMIm][ESO_4]. Diethyl sulfate (127 mmol) was added dropwise to a solution of 1-methyl imidazolium (127 mmol) in toluene (50 mL) cooled in an ice-bath under argon at a rate to maintain the reaction temperature below 40 ºC (exothermic reaction). The reaction mixture was stirred at room temperature for 1 h (the progress of the reaction was monitored by thin layer chromatography using 0.2 mm layer aluminum oxide N/UV254 and ethyl acetate + 25 % hexane as eluent). The upper organic phase of the resulting mixture was decanted, and the lower ionic liquid phase was washed with ethyl acetate (3 x 15 mL). After washings, the remaining ethyl acetate was removed by heating under reduced pressure to afford [EMIm][ESO_4] in high yield (92 %) and more than 99 % of purity. Its structure was determined by ^{1}H, ^{13}C NMR spectroscopy and confirmed by comparison with previously described data[29]. The RMN spectra for this compound and the NMR peaks position are included in the ESI.

1-ethyl-3-methylimidazolium decyl sulfate [EMIm][DSO_4]. Methanesulfonic acid (4.2 mmol) was added dropwise to a solution of 1-decanol (84 mmol) and [EMIm][ESO_4] (42 mmol) and the ternary mixture was stirred at 40 ºC for 8h. The ethanol formed in the reaction process was continuously evaporated by vacuum distillation. The reaction progress was monitored by ^{1}H-NMR spectroscopy. After the reaction was finished, the mixture was neutralized with an aqueous solution of NaOH 1 M. A white precipitate of sodium methyl sulfonate was formed and filtered. The liquid phase was then extracted with tert-butyl methyl ether (3 x 25 mL) in order to remove the excess of 1-decanol. Finally, the obtained [EMIm][DSO_4] was concentrated by rotary evaporation and dried by heating at 80 ºC and stirring under high vacuum ($2\cdot10^{-1}$ Pa) for 24 h to afford a crystalline solid in high yield (97 %). Its purity was estimated by ^{1}H NMR (400 MHz) and high resolution mass spectrometry (MS) showing to be more than 99% as observed in the spectra and peak position data given in the ESI. Electrospray MS (micrOTOF Focus) m/z (%): 807 $[(C_6H_{11}N)_3(C_{10}H_{21}O_4S)_2]^+$ (68), 460 $[(C_6H_{11}N)_2(C_{10}H_{21}O_4S) + 1]^+$ (26), 459.2997 $[(C_6H_{11}N)_2(C_{10}H_{21}O_4S)]^+$ (calc. for $C_{22}H_{43}N_4O_4S$: 459.3000, 100).

The final water content of the measured pure compound was about 1480 ± 60 ppm obtained from a Mettler Toledo C20 Coulometric Karl-Fischer titrator. Finally, note that the molar mass, M, of [EMIm][DSO_4] is equal to 348.45 g/mol.

Physical Properties

The ionic conductivity, the density and the viscosity of the pure sample and the first magnitude in two hydrated ones with 10 $_{wt}$% (x_{IL} = 0.317) and 39 $_{wt}$% of water (x_{IL} = 0.317), were experimentally measured. Mixtures where done by mass using a Gram ST510 balance which has an accuracy of ± 0.01 g. Ionic conductivity was measured with a CRISON GLP 31 conductivimeter (which uses a

constant ac current of 500 Hz) in an isothermal basis. Thus, the sample was left at least 15 minutes at each temperature before measuring it, and up to 3 hours in the liquid to crystal solid transition in the different phase transitions. The samples were thermostated using a Julabo 25 thermal bath with an uncertainty of 0.1 ºC. The experimental relative uncertainties of the ionic conductivity were less than 0.5 % of the measured value, being the repeatability better than 3%. Density and viscosity where simultaneously measured using a Stabinger Anton Paar SVM3000 viscodensimeter with a Peltier cell that allows choosing temperature with an uncertainty of 0.02 ºC, but a reproducibility of 0.1 ºC was assumed. The main advantage of this apparatus is that we can measure all viscosity range (from 0.2 up to 20,000 mPa·s) in continuo, without changing any part of it. The precision for the viscosity measured is better than 0.1 % and repeatability lower than 2 %. Moreover, density value is corrected from viscosity influence automatically, which is very important for very viscous samples as that measured here. Precision in density values is 0.5 $kg \cdot m^{-3}$ and its repeatability is about 1 $kg \cdot m^{-3}$. These measurements are also performed in the isothermal basis described above. Obviously, in the rigid-gel state a rheometer is needed to know its viscoelastic properties. As observed previously for $[EMIm][OSO_4]$[2], between the liquid and the rigid-gel state, the hydrated sample is in a stable intermediate liquid crystalline (called quasi-gel) state in an interval of some degrees Celsius. The different states where obtained by naked eye, proving the sample fluidity after each conductivity measurement.

In addition, these other instruments have been used to characterize the samples: Humidity grade of the atmosphere has been measured using a Kestrel 3500 Pocket Weather Meter with an accuracy of ±3 % and resolution of 0.1 %. The thermo-gravimetric analysis (TGA) was performed using a NETZSCH STA 449F3 TGA with a heating rate of 5 ºC/min in air atmosphere. Mid-infrared spectra were recorded in the range 400 to 4000 cm^{-1} using a Bruker Vector 22 mid-infrared FT-IR spectrometer equipped with a Specac Golden Gate single-reflection diamond ATR accessory with KRS-5 optics. These data were obtained at a sample temperature of 22 ºC. X-ray spectra was obtained from a Bruker Kappa-APEX-II, equipped with a X-ray Mo tube ($\lambda(K_{\alpha 1})$ = 0.71073 Å) at 50 KV and 30 mA, and a 2D detector APEX-II. Finally, A BIOLAR PI Microscope was used to observe the microstructure of a drop of the sample open to the atmosphere. This microscope operates in a cross polarizing configuration. It was directly coupled to a CCD camera. Using a x10 objective the total field of view of the camera covers an area of 400x290 μm^2 (756x576 pixels) in the object plane.

Results and discussion

Synthesis

$[EMIm][DSO_4]$ was prepared from the ionic liquid 1-ethyl-3-methyl imidazolium ethyl sulfate, $[EMIm][ESO_4]$, by treatment with 1-decanol in an acidic medium. $[EMIm][ESO_4]$ was previously obtained by a direct alkylation of 1-methyl imidazolium with diethyl sulfate. The two steps of the full procedure are indicated in Figure 1.

Water Adsorption

The $[EMIm][DSO_4]$ is a viscous liquid or a crystalline solid at room temperature, depending on its thermal history as it is observed in Figure 2. Here two photographs of the same sample at 30 ºC are shown, at left coming from hot (liquid) and in the middle coming from cold (white crystal). The pure sample used has a water content of 1480 ± 60 ppm from Karl-Fisher tritation. The exclusive property of this IL is that it self-hydrates naturally if open to the ambient moisture and, about some minutes later, the liquid was transformed into a mesomorphic liquid crystalline rigid-gel as observed in Figure 2 at right, where a hydrated sample with 10 $_{wt}$% of water appears also at 30 ºC. To study the hygroscopic character of this IL, a sample of pure $[EMIm][DSO_4]$ was left in a sealed box on a Petri plate (shown in the sketch of Figure 3(a)) and the humidity grade was regulated into the box. After some hours at a given value, the sample was weighted and the mass excess was assumed to be the water adsorbed. As it was expected, the compound is very hygroscopic due to its alkyl-sulfate anion[30]. Results are shown in Figure 3(a), where the weight percentage of water is presented as a function of the box humidity grade. In the vapor saturated atmosphere the sample increased its weight to about 33 % (which represents 27 $_{wt}$% of water). Part of this water is deposited in the surface of the sample, giving place to a water film on it. We guess that the maximum amount of water that the compound really adsorbs into the bulk is about 17 $_{wt}$% (which means x_{IL} = 0.2; i.e., four molecules of water for each sulfate ion). As can be observed in Figure 3(a), the relationship between the water composition in $_{wt}$% and the humidity grade is roughly parabolic. The obtained deviations could be due to the elevated response time of the IL to adsorb or loose water compared to that of the hygrometer used. Once the sample is in the liquid crystalline rigid-gel state, its weight stays nearly constant opened to the atmosphere for 5 months, as observed in Figure 3(b), where the same sample as before was left open in the laboratory and weighted daily. It is important to note that the hydration process is completely reversible, as it is observed in Figure 3(c). Here the time evolution of the water percentage (at left) and water molar fraction (at right) vs. time for a completely hydrated sample (which had adsorbed water up to be the 27 $_{wt}$% of the sample) after leaving it in a dry box (with plenty of silica gel and a humidity grade below 10 %), is shown. In less than 24 h the IL loses all adsorbed water and its weight equals that it had five months ago (and obviously it transits back to liquid state). A complete phase diagram temperature-composition was made; it is shown in Figure 4, where dot symbols correspond to $[EMIm][DSO_4]$, while triangle ones correspond to $[EMIm][OSO_4]$, already published and included for comparison[1]. The transition temperature, T_G, denoted with the open symbols, is up to 60 ºC higher for the decyl than for the octyl sulfate at $x_{IL} \approx 0.2$ (which is the composition where T_{RG} is higher for both ILs). At 25 ºC the water content of $[EMIm][DSO_4]$ mixture must be roughly between 4 $_{wt}$% and 40 $_{wt}$% to have the sample in the rigid-gel state, which represents a water molar fraction between 0.6 and 0.9. In contrast, $[EMIm][OSO_4]$ is not in the rigid-gel state at any water composition at 25 ºC. Figure 4 also shows melting points, T_m (clear filled symbols) and solidification ones, T_S (dark filled ones) for compositions where those temperatures were above -25 ºC (the minimum temperature reached by the thermostatic bath used).

As observed, values for T_m and T_S are roughly the same for both ILs in the high diluted regime ($x_{IL} \leq 0.05$).

A thermal gravimetrical analysis, TGA, at 5 ºC/min heating rate on a sample of 63.5 mg, including 12 $_{wt}$% of water, was performed. It shows that sample weight is lost while heating, being dry at about 200 ºC. The onset of decomposition (or evaporation) appears at about 300 ºC. The corresponding curve appears in ESI file.

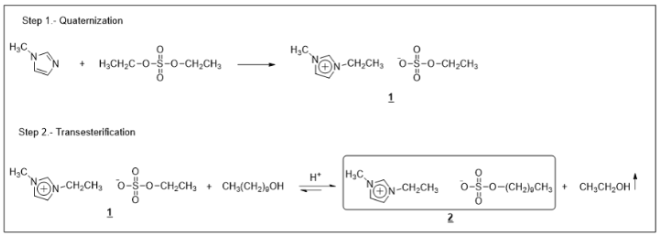

Figure 1. Synthetic procedure applied to prepare [EMIm][DSO_4].

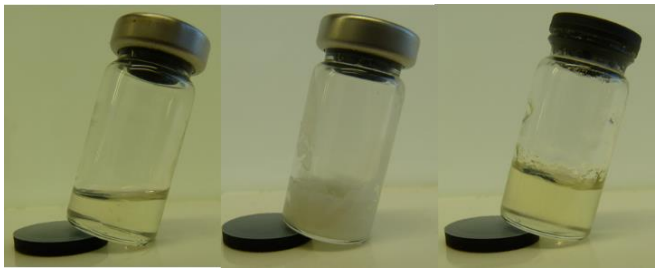

Figure 2. Photographs of the pure [EMIm][DSO_4] at 30 ºC. That at left coming from hot (liquid) and that in the middle from cold (white crystal). At right side appears a 10 $_{wt}$% hydrated sample at the same temperature in rigid-gel state.

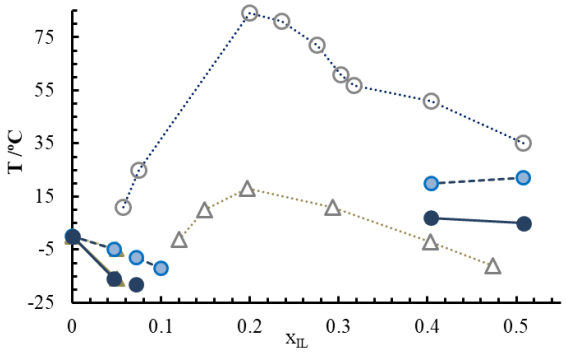

Figure 4. Phase diagram of [EMIm][OSO_4][1] (triangle symbols) and [EMIm][DSO_4] (dot ones). Open symbols represent the liquid to quasi-gel transition temperature, T_G, light filled ones the melting one, T_m, and dark filled symbols the solidification temperature, T_S.

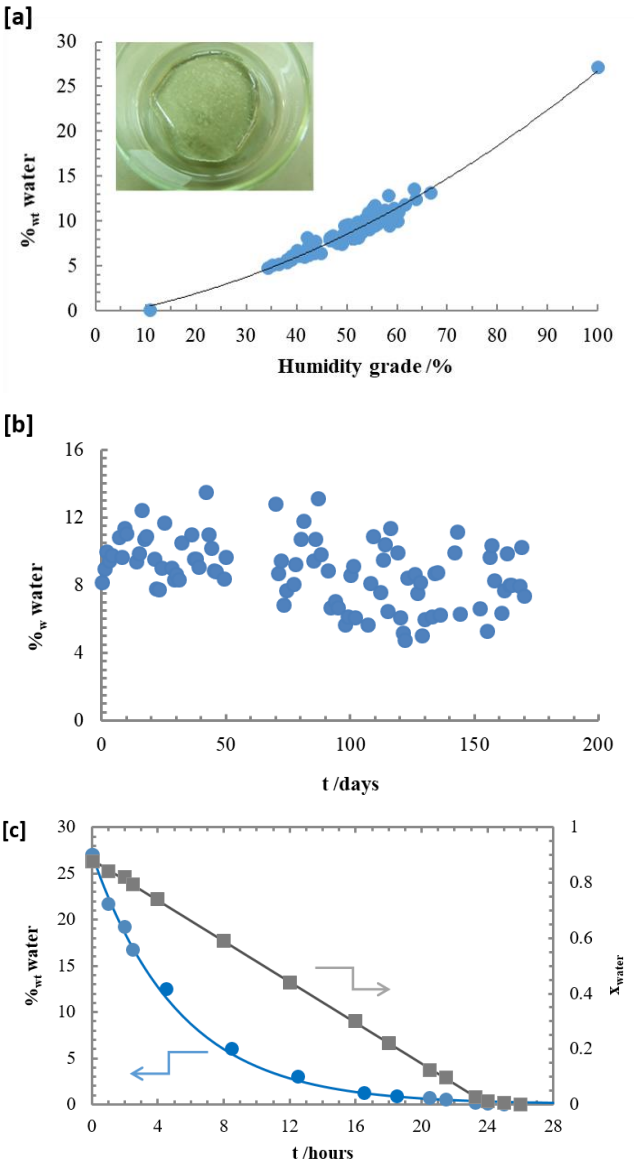

Figure 3. (a) Weight percentage of adsorbed water in function of the humidity grade percentage. Continuous line is the best quadratic fit. (b) Water content percentage variation with time after leaving the sample for 5 months open to the atmosphere. (c) Content of water with time in weight percentage (left) and water molar fraction (right) when a saturated hydrated sample is stored in a dry box. Curves are the best fit of a linear one for molar fraction and of an exponential one for weight percentage.

Microstructure

The Fourier Transformed Infrared (FTIR) spectra for the pure [EMIm][DSO_4] and the sample hydrated with 10 $_{wt}$% of water at room temperature (about 22 ºC) is shown in Figure 5. The obtained peaks indicate the presence of the [EMIm] cation (ring stretching at the wave number k = 1570 cm^{-1} and bending in k = 1450 cm^{-1})[31], and sulfate anion (stretching at k = 1140 and 990 cm^{-1}, and bending at k = 600 cm^{-1})[31]. In addition, the peaks corresponding to water (1650 cm^{-1} for bending and 3500 cm^{-1} for stretching)[32] can be also observed in the hydrated sample. Except for these last peaks, the position of all the other ones in the spectrographs of both samples are identical (being the height of the peaks, as usual, arbitrary).

Figure 6 shows the 1D X-ray diffractograms of a 7 $_{wt}$% hydrated sample of [EMIm] [DSO_4] (x_{IL} ~ 0.4) at different temperatures from 0 ºC to 80 ºC following the isothermal method explained above. When cooling, shown in Figure 6(a), the crystalline character appears abruptly between 5 and 7 ºC. When the sample is heated, as in Figure 6(b), the crystal phase begins to disappear at 5 ºC, but this phase change from crystal to the mesomorphic phase is progressive, and at 20 ºC a crystal signal is still present. The unit cell for the crystal phase, calculated from the data at 0 ºC, corresponds to a P2/m monoclinic class, with cell parameters *a* = 19.7 Å, *b* = 10.2 Å and *c* = 15.2 Å and angles $\alpha = \gamma = 90^o$ and $\beta = 115^o$. In Figure 6 two of the Debye circles obtained from X-ray diffraction are also included, on the left for the solid crystal (T = 0 ºC) and on the right for the rigid-gel state (T = 40 ºC). Only the coldest sample shows crystal diffraction pattern. The thermal hysteresis that suffers this IL is clearly observed in Figure 6. This effect is typical for the majority of pure ILs and it is also observed from ionic conductivity measurements[33]. From Figure 6 we can also conclude that 1D X-ray analysis does not reveal the microstructure of the rigid-gel state, being the diffractograms of this phase equal to that for the liquid (above 50 ºC for the sample used).

Figure 7 shows the temporal evolution and the microstructure formation through micrographs obtained with white polarized light microscopy of the pure sample when it is self-hydrated adsorbing moisture at room temperature. The observed microstructure (with clear striped cone forms) resembles that of a liquid crystal, being both patterns characteristic of a smectic (also called exatic) B phase[34], although more techniques must be used to be sure of the given mesostructure in the rigid-gel state. As we pointed out recently, this phase is probably due to two effects: first to the tendency to the formation of micelles of the long alkyl sulfate anions, with its head in the outer part forming H-bonds with the water molecules[35]; and second, to the chromonic character of the imidazolium ring, which tends to stack forming columns due to the interaction of the adjacent π clouds of these aromatic cations[11]. As published before[2], when thermal agitation is low enough, $T < T_G$, the long tubular micelles begins to bond forming hexagonal H_I mesostructures, the process is finished when $T < T_{RG}$, all micelles are packed and the sample does not flow at all under gravity, although ionic conductivity is preserved...

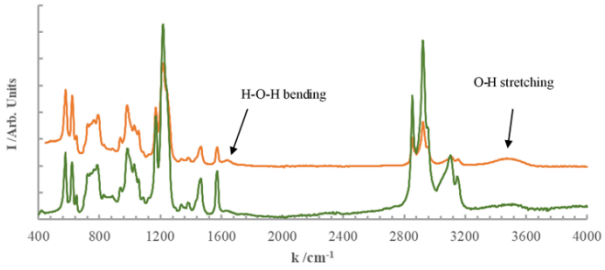

Figure 5. FTIR spectra of the pure [EMIm][DSO_4] (bottom green line) and that hydrated with 10 $_{wt}$% of water (top orange line) at 22 ºC.

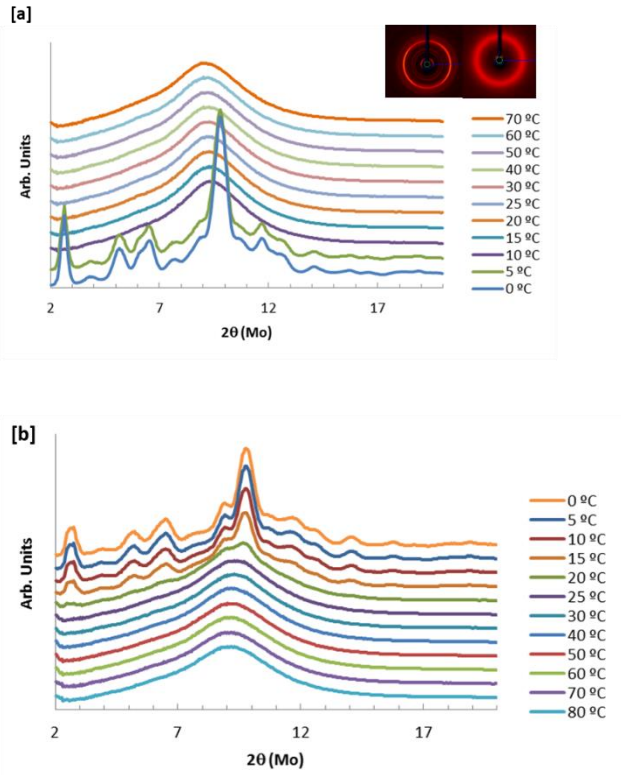

Figure 6. Mo ($\lambda(K_{\alpha 1})$ = 0.71073 Å) X-ray diffractogram of the hydrated [EMIm][DSO_4] with 7 $_{wt}$% of water at different temperatures: (a) Sample is cooling down. (b) Sample is warming up. Two 2D Debye circles for crystal (left) and gel (right) are included in (a).

The change in colour observed over time is due to a variation in the local birefringence of the sample[36]. The observed colour sequence, if compared to the Michel-Levy colour chart for ordered birefringent media[37], suggests an increase in birefringence associated with the slow incorporation of water into the structure. The change in birefringence may be due to modification of extreme, ordinary (n_o) and extraordinary (n_e), refractive index values of the domain and also to changes in the direction of the optical axis that involve changes in the velocity of the extraordinary wave (and so in the refractive index along the propagation direction of this wave), even though did not change. The direction of the optical axis is determined by the orientation of the amphiphilic IL anions, which undergoes important

changes during the process of water absorption. However, the effect of the modification of the thickness of the open sample during the incorporation of water must be also considered as well as a possible modification of the optical properties of the surface associated to the adsorption of water molecules at the air-liquid interface.

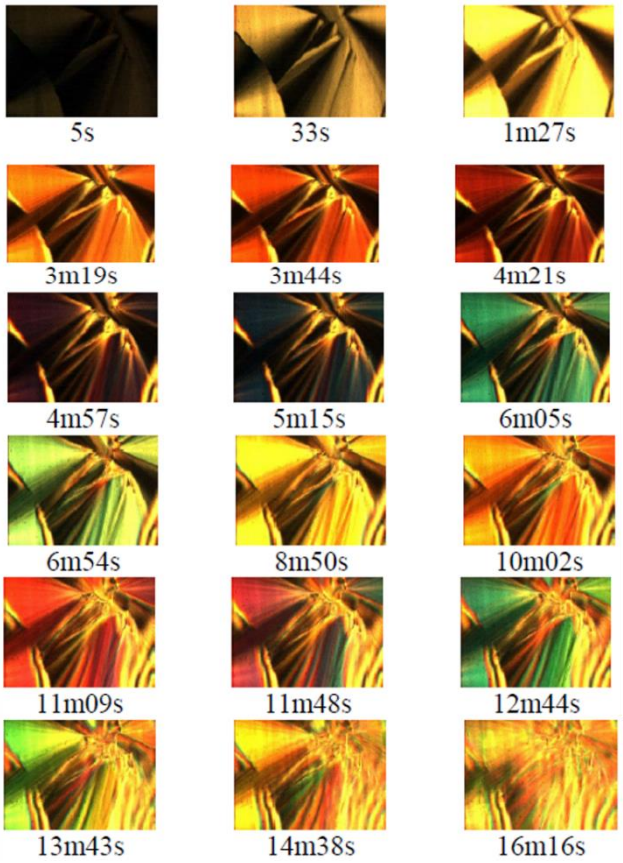

Figure 7. Temporal evolution of a drop of [EMIm][DSO_4] left in the microscope at room temperature while adsorbing water from moisture through polarized white light microscopy. Scale of all photographs is 400 x 290 μm^2.

In relation to this, one can observe that from 6 minutes, the previous well defined structure is deformed and less sharply domains appear. We believe that a thin film of adsorbed water may be the cause of the distortion, since it induces new boundary conditions that force the ordering of the IL anion chains in a slab close to the free interface. In addition to the effect of water absorption on the birefringence, one must also consider the variation of the dielectric constant response of the liquid regions of the gel sample associated to local fluctuations of the ionic concentration upon the process of water addition[38], which leads to an increase of the dielectric constant with water concentration. Similar domains are also observed when the aqueous mixture is sandwiched between two microscope slices.

Physical properties

As mentioned above, temperature behaviour of some physical properties (ionic conductivity, density and viscosity) of the pure [EMIm][DSO_4] sample were measured, and also the ionic conductivity of two hydrated ones: with x_{IL} = 0.317 (10 $_{wt}$% of water) and with x_{IL} = 0.075 (39 $_{wt}$% of water). The results for the ionic conductivity between 0 ºC and 100 ºC for the three samples are plotted in Figure 8, while Table S1 shows the corresponding numerical data (see ESI). As expected from previous results[39], ionic conductivity increases greatly when the IL is mixed with water (about one order of magnitude higher for sample with 10 $_{wt}$% water content, and two orders for that with 39 $_{wt}$%, both respecting the pure one). As usual, in the liquid and rigid-gel states the temperature behaviour of the ionic conductivity follows a Vogel Tamman Fulcher (VTF) like curve for the three samples measured[1,2,40], which reads

$$\kappa = \kappa_\infty e^{-B_\kappa/(T-T_V)} \quad (1)$$

where the parameters have the following physical meaning: κ_∞ is the limiting value of ionic conductivity at infinite temperature, B_κ is related to the activation energy for the ion hopping, while T_V is the so called Vogel's temperature, which is a little bit higher than the glass transition one[40]. These results are very similar to those recently measured for [EMIm][OSO_4][41].

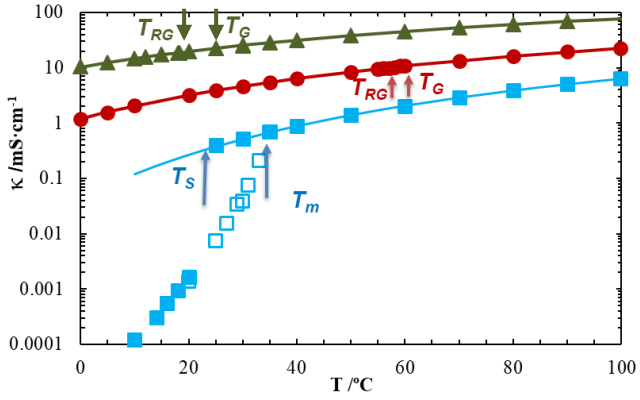

Figure 8. Three series showing temperature behaviour of the ionic conductivity of the pure [EMIm][DSO_4] (blue square, when cooling with open symbols and while heating with open ones); hydrated with 10 $_{wt}$% of water (red dots); and 39 $_{wt}$% of water (green triangles). Vertical arrows mark, for the pure sample, its melting (T_m) and solidification (T_S) temperatures. For hydrated samples arrows show liquid to quasi-gel (T_G) and to rigid-gel (T_{RG}) transition temperatures. Solid lines are the best fit of a VTF equation (1) of the corresponding experimental data above melting temperature.

The resulting best fitted curves are plotted in Figure 8, being the obtained fitting parameters given in Table 1, with the corresponding standard deviation of each fit, *s*. The pure sample presents the typical hysteresis loop, due to the different value

of its melting and solidification temperatures, also observed above with the X-ray diffraction. That loop marks the melting point (at T_m = 33 ºC obtained increasing temperature) and the crystallization one (at T_S = 22 ºC when temperature is decreased), being both temperatures marked with a blue arrow in Figure 8. As discussed before, this fact is due to the ability of ILs to be in an undercooled stable liquid state (or rigid-gel for our aqueous mixtures)[1,33]. To know if the undercooled liquid is a transitory state, we left the pure sample at 30 ºC (from liquid state) more than 24 hours, and later at the same temperature but from solid crystal state.

Table 1. Fitting parameters of the VTF-like equations (1) and (2) for the ionic conductivity of the pure and two hydrated [EMIm][DSO_4] samples, and for viscosity of the pure one.

Sample	η_∞ /mPa·s	B_η /K^{-1}	T_η /K	s /mPa·s	κ_∞ /S·m^{-1}	B_κ /K^{-1}	T_κ /K	s /S·m^{-1}
Pure	0.0924	1248.3	160.6	0.036	31.3	691	195.4	0.002
10 wt%	-	-	-	-	45.3	593	172.3	0.010
39 wt%	-	-	-	-	72.1	475	161.3	0.013

Each sample was in the same state as originally the following day, as shown in Figure 2 (left and middle photographs). For the hydrated samples we observe that the ionic conductivity does not change its temperature behaviour in the transition between the isotropic (liquid) to mesomorphic (quasi-gel) states (at T_G = 60 ºC for sample 10 $_{wt}$% hydrated and T_G = 25 ºC for that with 39 $_{wt}$% water, both for increasing and decreasing temperatures). Also, no change in ionic conductivity VTF behaviour has been observed for the quasi-gel to rigid-gel transitions (at T_{RG} = 57 ºC for sample 10 $_{wt}$% hydrated and T_{RG} = 19 ºC for that with 39 $_{wt}$% of water, also both for increasing and decreasing temperatures). This behaviour, also observed for aqueous mixtures of [EMIm][OSO_4], is in contrast with the drop of ionic conductivity observed for other soft matter systems based in ILs, where it is observed a sharp drop of this magnitude when quasi-solid phase appears[25,42]. The absence of conductivity change in the isotropic-mesomorphic transition does not adapt to the usual theory of ionic charge transport given in textbooks of electrochemistry, which implies an ionic displacement between both electrodes following the Nerst-Einstein equation. A 1D cationic mechanism of charge transport[43] seems to be more plausible for the hydrated sample both in rigid-gel and also in liquid states. This charge transport mechanism has been proposed by us for the parent compound [EMIm][OSO_4][2], although more experiments are needed to completely elucidate its deep nature.

In Figure 9 the temperature dependence of the viscosity (solid symbols in the left axis) and density (open ones in the right axis) of the pure [EMIm][DSO_4] in liquid state are shown. The corresponding measured experimental values are given in Table S2 of ESI. As observed, density follows a linear behaviour with temperature as usual, thus

$$\rho\ /\mathrm{kg\cdot m^{-3}} = 1117.1 - 0.663\ T\ /^{\circ}\mathrm{C}\ . \qquad (2)$$

Viscosity follows a VTF-like curve as the majority of ILs do[2,41].

$$\eta = \eta_\infty e^{B_\eta/(T-T_0)} \quad , \qquad (3)$$

where η_∞ is the limit viscosity at infinite temperature, B_η is proportional to the activation energy of ions to flow and T_0 is related to the glass transition temperature.

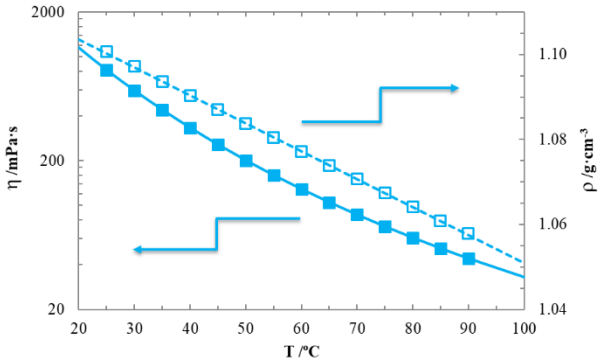

Figure 9. Viscosity (solid symbols) and density (open ones) vs. temperature of the pure sample. Lines are the best fits of a straight line for density and VTF equation (3) for viscosity.

The corresponding curves are plotted in Figure 9, while the corresponding fitting parameters are included in Table 1, with its standard deviation. Results agree with those recently published for other members of the [EMIm] alkyl sulfate family[41]. We have not measured viscosity for the hydrated samples because in the mesomorphic states our apparatus is not appropriate. Comparing fluidity (null at laboratory conditions) and ionic conductivity curves in the rigid-gel state of the hydrated samples, it can be deduced that charge mobility is completely independent of fluidity, which contradicts Walden's rule, followed by the majority of electrolytes (including ILs), that relates those two magnitudes[2,41,44]. Similar decoupling of ionic conductivity from structural dynamics was recently observed for polymerized ionic liquids[17,25,43]. In those papers authors suggest that the anion moves freely in the rigid network formed by the cation (which is the moiety with long alkyl chain in the IL compounds they study). In a similar way, the long alkyl chained [DSO_4] anions do not have mobility enough to transport charge due to their size, so this is carried meanly by the much smaller [EMIm] cations, even in the pure compound, as it was suggested previously for alkyl sulfate based ILs with chains longer than seven carbon atoms[41]. When water is added the anions get fixed forming micelles due to its lyotropic character (which forms a maximum of four H-bonds between each of the four oxygen atoms of the sulfate with a water molecule[35]) which take a tubular form due to the chromonic character of imidazolium cations[11]. Thus, while anions are fixed, cations can still move on the crust of such tubular micelles due to their poorly coordination with anions through the water molecules in between. When mesomorphic state is formed, those micelles aggregate forming a liquid-crystalline H_I mesostructure[2,34] random oriented in micro-domains. Unexpectedly, charge

transport of cations is unaltered and so the ionic conductivity does not change its behaviour in the phase transition. In the pure sample, when crystallization is reached below T_S, [EMIm] cations get anchored in an ionic network forming a solid crystal. As a consequence, the ionic conductivity value sharply decreases (more than an order of magnitude). The crystallization process is quite slow and so, to obtain accurate values of the measured ionic conductivity, we must wait a long time to stabilize the sample (up to three hours near but below T_S). Diffusion measurements of both anions and cations in the isotropic and mesomorphic states would surely clarify the 1D charge transport model suggested.

Conclusions

Synthesis and physical properties of a new ionic liquid, 1-ethyl-3-methylimidazolium decyl sulfate, is described. This compound has the ability of transiting to a rigid-gel state at room temperature when it naturally adsorbs moisture from atmosphere. The adsorbed water depends on the humidity grade (h.g.) but it is about 10 $_{wt}$% in the hydrated sample at laboratory conditions (h.g. about 60%). The synthesis process as well as the microstructure characterization, using NMR, MS, FTIR, X-ray diffraction, TGA and polarized micrographs, are presented. Also we include the temperature-composition phase diagram of this compound. Finally, experimental measurements of its ionic conductivity, density and viscosity vs temperature are also included for the pure sample. The ionic conductivity of two different aqueous mixtures is also included. A mesostructure model is presented to explain data obtained. This compound reopens the important question about the relationship between charge and mass transport in quasi-solid conductors. In rigid-gel state fluidity is null while conductivity is relatively high, contrarily to what happens for the majority of ILs (and its aqueous mixtures) in liquid state where these two last magnitudes are related through Walden rule.

Acknowledgments

The authors are grateful to the UDC technician Manuel Cabanas for some of the great quality measurements he performed. Also, we acknowledge to Susana Yáñez for resolving the X-ray data. O.C. acknowledge Ana Gras for her continuous support. This work was financed by MINECO from Spanish Government (Grants Nº MAT2014-57943-C3-1-P, MAT2014-57943-C3-2-P, MAT2014-57943-C3-3-P and DPI2012-38841-C02-02), by the European Union (COST Action CM 1206) and by the Galician Network on Ionic Liquids, REGALIs (CN 2014/015). Research projects have been co-financed by the European Regional Development Fund (FEDER).

References

1. O. Cabeza, J. Vila, E. Rilo, M. Domínguez-Pérez, L. Otero-Cernadas, E. López-Lago, T. Méndez-Morales, and L.M. Varela, *J. Chem. Thermodyn.*, 2014, **75**, 52.
2. O. Cabeza, L. Segade, M. Domínguez-Pérez, E. Rilo, S. García-Garabal, D. Ausín, A. Martinelli, E. López-Lago and L.M. Varela, *J. Chem. Thermodyn.*, 2017, **112**, 267.
3. R.K. Rogers, K.R. Seddon (Eds.), *Ionic Liquids, Industrial Applications to Green Chemistry,* ACS Symp. Series 818, Am. Chem. Soc., Washington, 2002.
4. T. Inoue, H. Ebina, B. Dong and L. Zheng, *J. Colloid Interface Sci.*, 2007, 314, 236.
5. S. T. Hyde, Handbook of Applied Surface and Colloid Chemistry, 2002, 2, 299.
6. M. A. Firestone, J. A. Dzielawa, P. Zapol, L.A. Curtiss, S. Seifert and M. L. Dietz, *Langmuir*, 2002, 18, 7258.
7. H. Kaper and B. Smarsly, *Z. Phys. Chem.*, 2009, 220, 1455.
8. O. Russina, L. Gontrani, B. Fazio, D. Lombardo, A. Triolo and R. Caminiti, *Chem. Phys. Lett.*, 2010, 493, 259.
9. O. Russina and A. Triolo, *Faraday Discuss.*, 2012, 154, 97.
10. O. Russina, F. Lo Celso, N. V. Plechkova and A. Triolo, *J. Phys. Chem. Lett.*, 2017, 8, 1197.
11. A.F. Kostko, B.H. Cipriano, O.A. Pinchuk, L. Ziserman, M.A. Anisimov, D. Danino and S.R. Raghavan. *J. Phys. Chem. B*, 2005, 109, 19126.
12. M. Armand, F. Endres, D.R. MacFarlane, H. Ohno and B. Scrosati, *Nature Materials*, 2009, **8**, 621.
13. H. Ohno (Ed.), Electrochemical aspects of Ionic Liquids, Wiley and Sons, New Jersey, 2011.
14. M. Díaz, A. Ortiz, and I. Ortiz, *J. of Membrane Science*, 2014, **469**, 379.
15. T.-Y. Wu, S.-G. Su, S.-T. Gung, M.-G. Lin, Y.-C. Lin and C.-A. Lai, *Electrochimica Acta*, 2010**, 55**, 4475.
16. A. Noda and M. Watanabe, *Electrochimica Acta*, 2000, **45**, 1265.
17. P. Vidinha, N.M.T. Lourenço, C. Pinheiro, A.R. Brás, T. Carvalho, T. Santos-Silva, A. Mukhopadhyay, M.J. Romaô, J. Parola, M. Dionisio, J.M.S. Cabral, C.A.M. Afonso and S. Barreiros, *Chem. Commun*., 2008, 5842.
18. S. Doherty, J.G. Knight, J.R. Ellison, P. Goodrich, L. Hall, C. Hardacre, M.J. Muldoon, S. Park, A. Ribeiro, C.A. Nieto de Castro, M.J. Lourenço and P. Davey, *Green Chem*., 2014, **16**, 1470.
19. A. Sharma, K. Rawat, P.R. Solanki, H.B. Bohidar, *Int. J. of Biological Macromolecules*, 2017, **95**, 603.
20. K. Rawat, J. Pathak, H.B. Bohidar, *Soft Matter*, 2014, **10**, 862.
21. A. Hussain, A.T.S. Semeano, S.I.C.J. Palma, A.S. Pina, J. Almeida, B.F. Medrado, A.C.C.S. Pádua, A.L. Carvalho, M. Dionísio, R.W.C. Li, H. Gamboa, R.V. Ulijn, J. Gruber, A.C.A. Roque, *Adv. Funct. Mater.*, 2017, **27**, 1700803.
22. N. Yoshimoto, T. Shirai and M. Morita, *Electrochimica Acta*, 2005, **50**, 3866.
23. M. Cai, Y. Liang, F. Zhou and W. Liu, *J. Mater. Chem*., 2011, **21** 13399.
24. M. Bielejewski, M. Ghorbani, M.A. Zolfigol, J. Tritt-Goc, S. Noura, M. Narimani, M. Oftadeh, *RSC Adv.*, 2016, **6**, 108896.
25. A.S. Shaplov, R. Marcilla and D. Mecerreyes, *Electrochimica Acta*, 2015, **175**, 18.
26. Patent Nº ES201400476. Priority Date 10/06/2014.
27. M. Ghorbani, S. Noura, M. Oftadeh, E. Gholami, M.A. Zolfigol, *RSC Adv.*, 2015, **5**, 55303.
28. S. Mahajan and I. P. Singh, *Magn. Reson. Chem*., 2013, **51**, 76.
29. E. Gómez, B. González, N. Calvar, E. Tojo and A. Domínguez, *J. Chem. Eng. Data*, 2006, **51**, 2096.
30. S. Cuadrado-Prado, M. Domínguez-Pérez, E. Rilo, S. García-Garabal, L. Segade, C. Franjo and O. Cabeza. *Fluid Phase Equilibria*, 2009, **278**, 36.

31. O. Hofft, S. Bahr, and V. Kempter, *Langmuir*, 2008, **24**, 11562.
32. S.C.B. Myneni, S.J. Traina, G.A. Waychunas, T.J. Logan, *Geochimica et Cosmochimica Acta*, 1998, **62**, 3499.
33. J. Vila, B. Fernández-Castro, E. Rilo, J. Carrete, M. Domínguez-Pérez, J.R. Rodríguez, M. García, L.M. Varela and O. Cabeza, *Fluid Phase Equilib.*, 2012, **320**, 1.
34. P.J. Collings, M. Hird. Introduction to Liquid Crystals: Chemistry and Physics. CRC Press, London, 1997.
35. T. Singh, M. Drechsler, A.H.E. Müeller and I. Mukhopadhayay, *Phys. Chem. Chem. Phys.*, 2010, **12**, 11728.
36. M. Born**,** E. Wolf, *Principles of Optics (4th.ed.)* Pergamon Press 1970.
37. M.-Lévy, *Eur. J. Mineral*. 2013, **25**, 5.
38. A. Levy, D. Andelman and H. Orland, *Phys. Rev. Lett.*, 2012, **108,** 227801.
39. J. Vila, P. Ginés, E. Rilo, O. Cabeza and, L.M. Varela, *Fluid Phase Equilib.*, 2006, **247**, 32.
40. J. Vila, P. Ginés, J.M. Pico, C. Franjo, E. Jiménez, L.M. Varela and O. Cabeza. *Fluid Phase Equilibria*, 2006, **242**, 141.
41. S. García-Garabal, J. Vila, E. Rilo, M. Domínguez-Perez, L. Segade, E. Tojo, P. Verdía, L.M. Varela and O. Cabeza, *Electrochimica Acta*, 2017, **231**, 94.
42. M. Figueira-González, V. Francisco, L. García-Río, E.F. Marques, M. Parajó and P. Rodríguez-Dafonte. *Phys. Chem. B*, 2013, **117,** 2926.
43. H. Shimura, M. Yoshio, K. Hoshino, T. Mukai, H. Ohno, and T. Kato, *J. Amer. Chem. Soc.*, 2008, **130**, 1759.
44. C.A. Angell, Y. Ansari and Z. Zhao, *Faraday Discuss*, 2012, **154**, 9.
45. J. R. Sangoro, C. Iacob, A. L. Agapov, Y. Wang, S. Berdzinski, H. Rexhausen, V. Strehmel, C. Friedrich, A. P. Sokolov and F. Kremer, *Soft Matter*, 2014, **10**, 3536.